LAVA Contribution to HiLiftPW-3

James Jensen, Marie Denison, Gerrit Stich, Jeff Housman, and Cetin Kiris

Computational Aerosciences Branch

NASA Ames Research Center

PID 033

3rd High Lift Prediction Workshop

Denver, CO June 3-4, 2017

Summary of cases completed:

- LAVA, Overset Structured, SA-QCR2000

Case	Alpha=8, Fully turb, grid study	Alpha=16, Fully turb, grid study
1a (full gap)	yes	yes
1c (partial seal)	yes	yes

Case	Polar, Fully turb	Polar, specified transition	Polar, w transition prediction
2a (no nacelle)	yes	no	no
2c (with nacelle)	yes	no	no

- LAVA, Unstructured Polyhedral, SA

Case	Polar, Fully turb	Polar, specified transition	Polar, w transition prediction
2c (with nacelle)	yes	no	no

Case	2D Verification study
3	yes

LAVA Framework

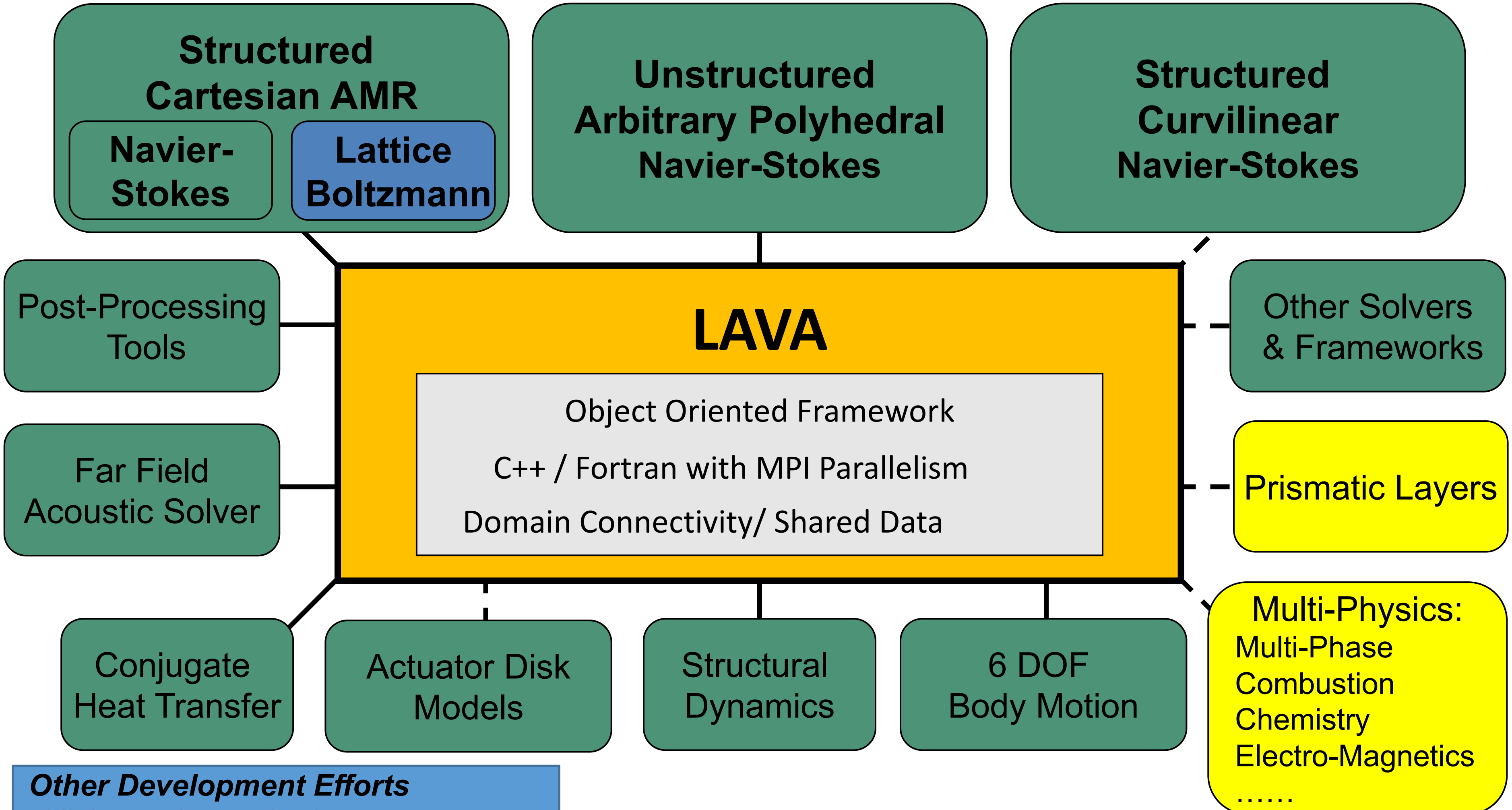

Other Development Efforts
- Higher order methods
- Curvilinear grid generation
- Wall modeling
- LES/DES/ILES Turbulence
- HEC (optimizations, accelerators, etc)

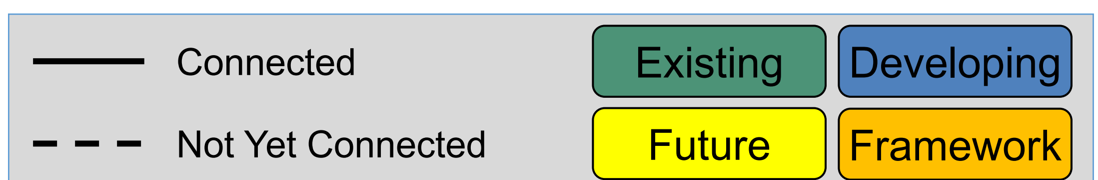

Kiris at al. AST-2016 and AIAA-2014-0070

LAVA Computational Grid Paradigms

Structured Cartesian AMR

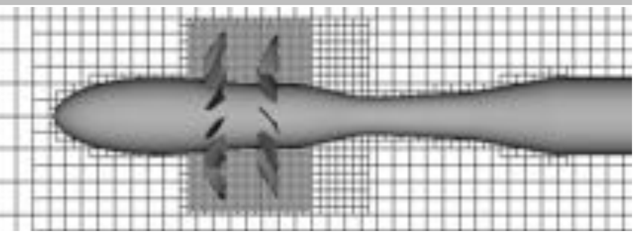

- Essentially no manual grid generation
- Highly efficient Structured
- Adaptive Mesh Refinement (AMR)
- Low computational cost
- Reliable higher order methods
- Non-body fitted -> Resolution of boundary layers inefficient

Unstructured Arbitrary Polyhedral

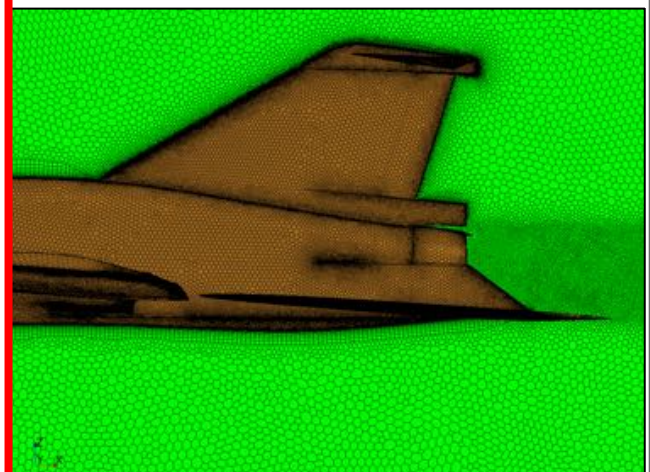

- Partially automated grid generation
- Body fitted grids
- Grid quality can be challenging
- High computational cost
- Higher order methods yet to fully mature

Structured Curvilinear

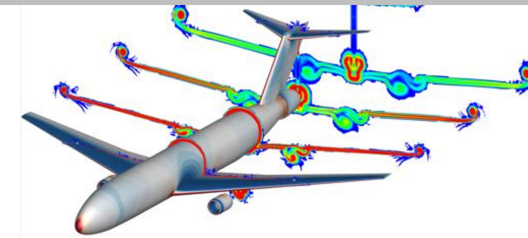

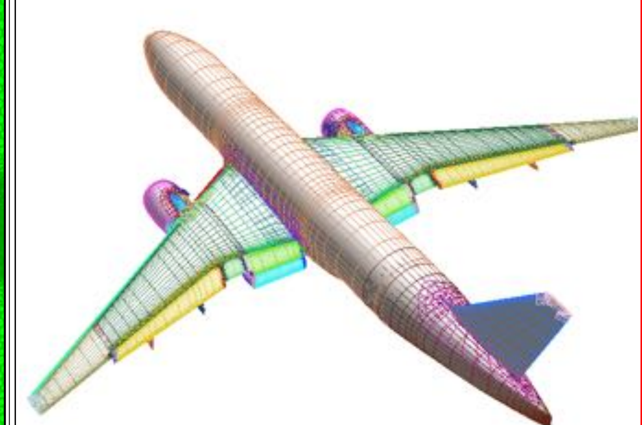

- High quality body fitted grids
- Low computational cost
- Reliable higher order methods
- Grid generation largely manual and time consuming

LAVA Solver Details

Unstructured Arbitrary Polyhedral	***Structured Curvilinear***

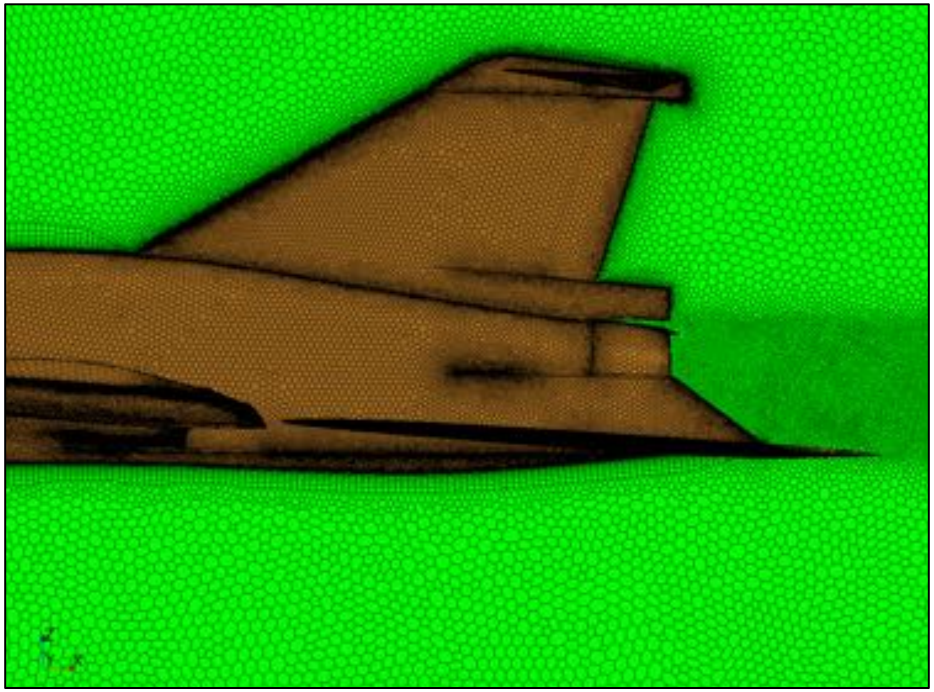

- 2^{nd} Order
- Cell Centered
- MUSCL Scheme
- AUSMPW+ Flux Function
- SA Turbulence Model

All simulations are cold starts with no CFL ramping

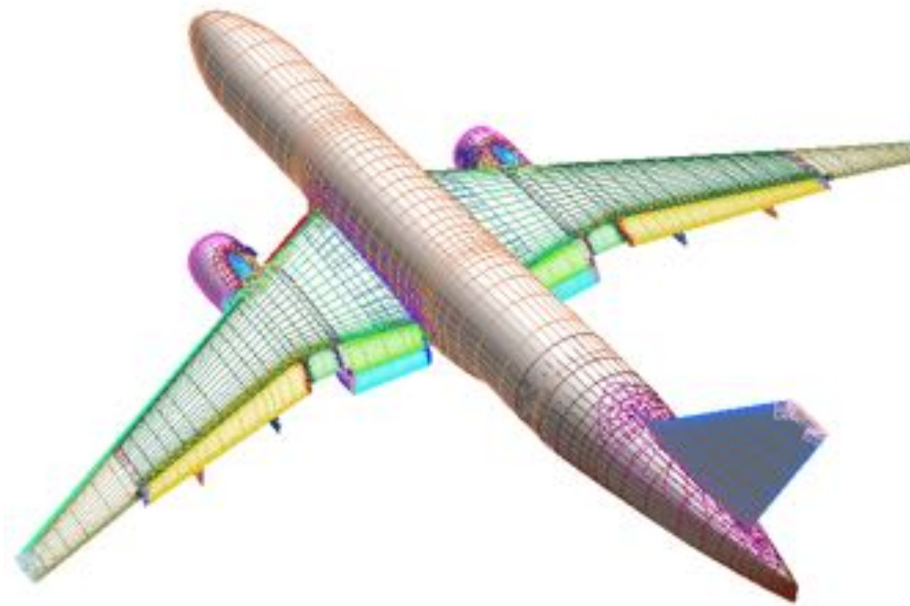

- 3D Structured Curvilinear RANS solver
- 2^{nd} order accurate Modified Roe Flux Difference Splitting for the convective terms
- 2^{nd} order central differencing for the viscous terms
- SA turbulence model with QCR-2000 for viscous flux tensor

Brief overview of grid system(s)

Grid System	Case(s)	If committee grid, report any problems/issues If user grid, reason for generating grid system
Committee (Grid A, Structured Overset)	1a and 1c	Observed solution decoupling in unexpected areas of the grid
Committee (Grid A, Structured Overset)	2a and 2c	Used custom domain connectivity with committee grids
User (Unstructured Polyhedral)	2c	Custom generated with different wake refinements

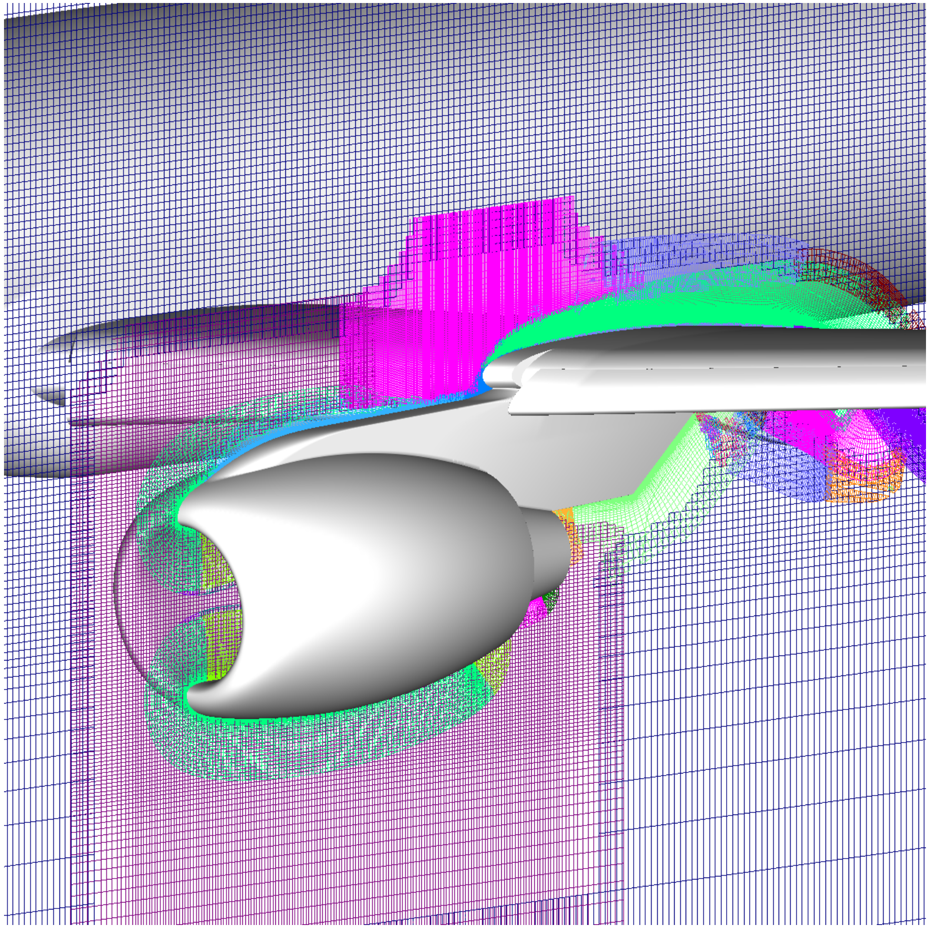

Overset Grid for Case 2c

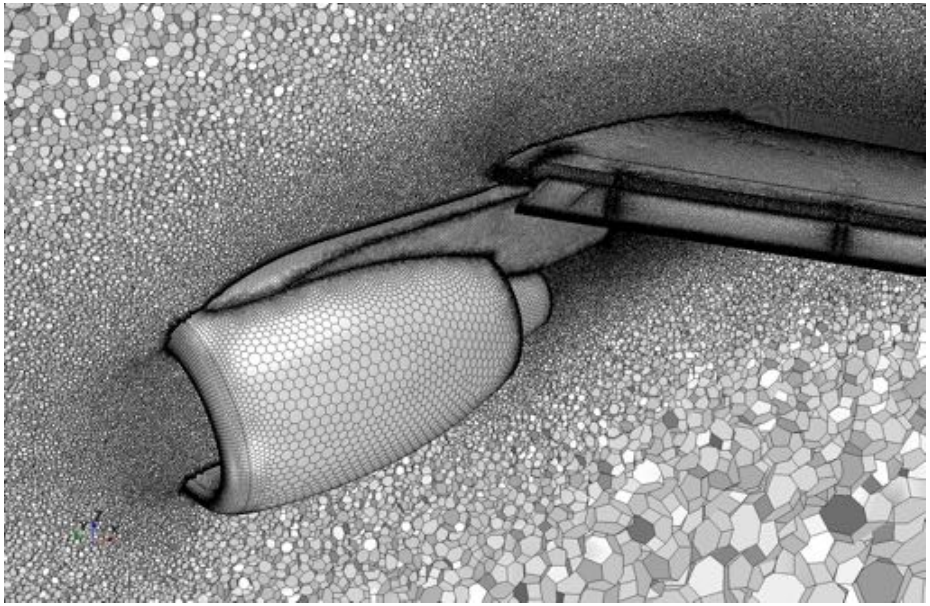

Unstructured Grid for Case 2c

Generating the Overset Structured Committee Grids for Case 2

- Generated with the Chimera Grid Tools (CGT)
- The grid was generated as a medium grid using the parameters from the gridding guidelines document provided by the committee
  - Trailing edge had 25 points instead of the 9 specified in the document
  - Spanwise spacing at the root and tip of elements was based on local cell sizes
  - Used separate wake meshes rather than a region of uniform spacing in the volumes

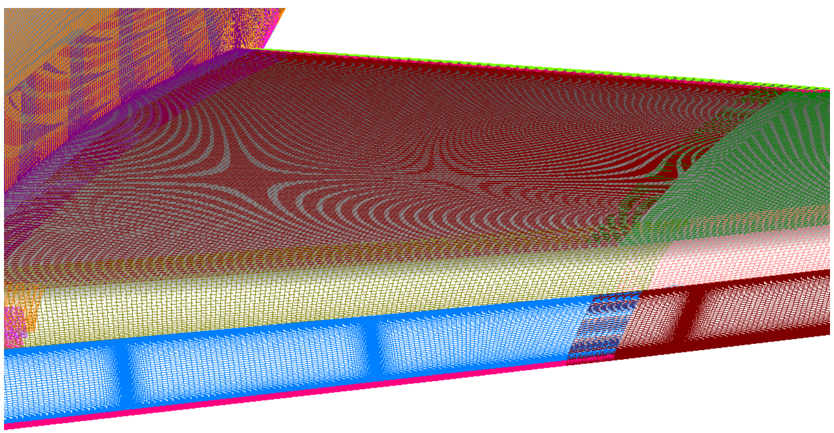

Case 2a

Case 2c

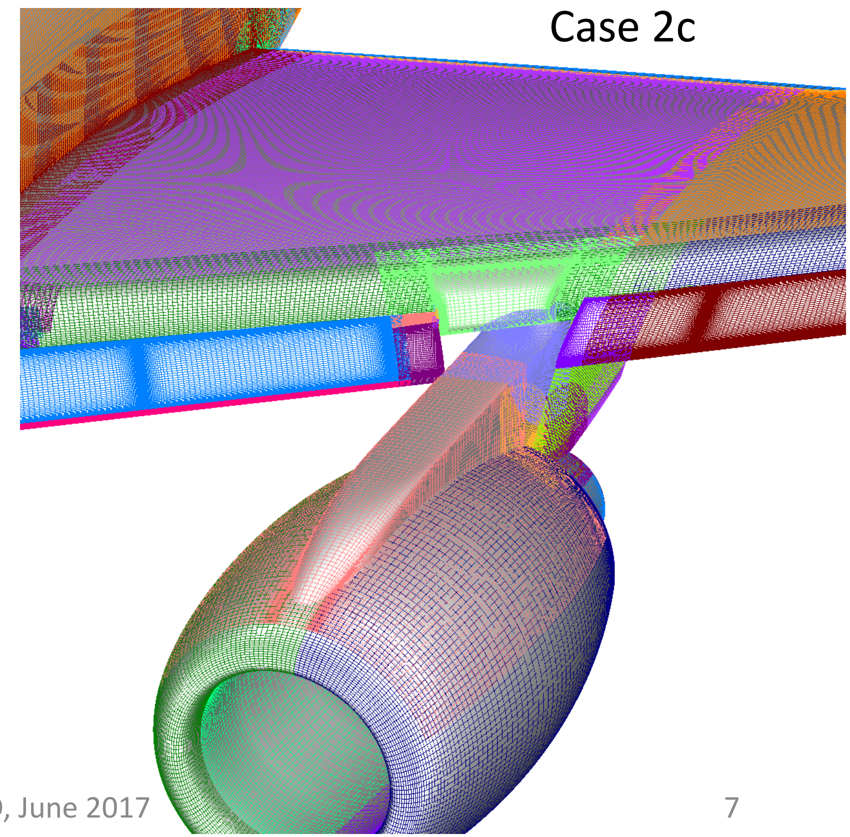

Reasoning Behind Wake Grids

- Original plan was to generate an wake grid based on the streamlines
- The streamlines vary greatly with angle of attack so the streamline based wakes were not general
- Decided to use a "geometric" based wake grid

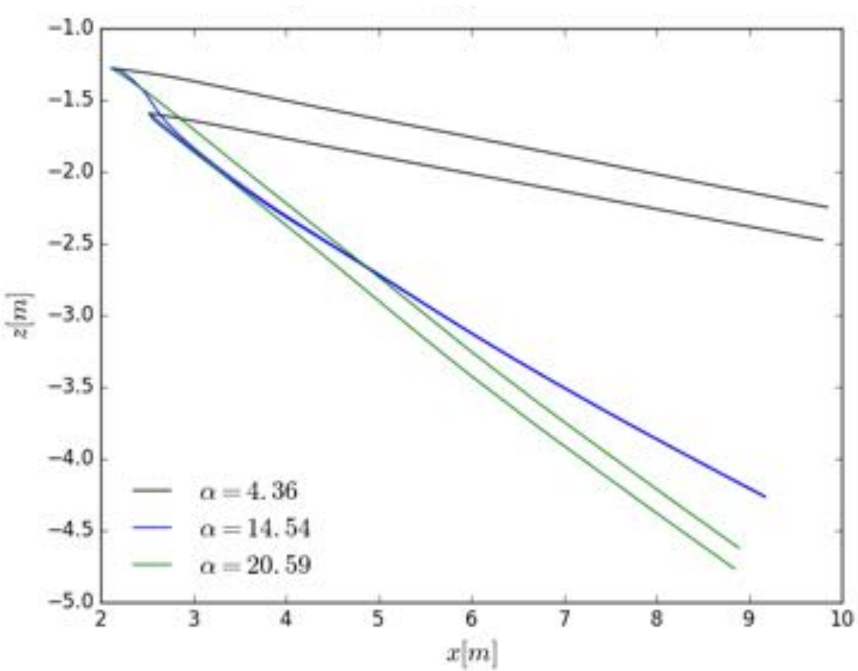

Wake Streamlines

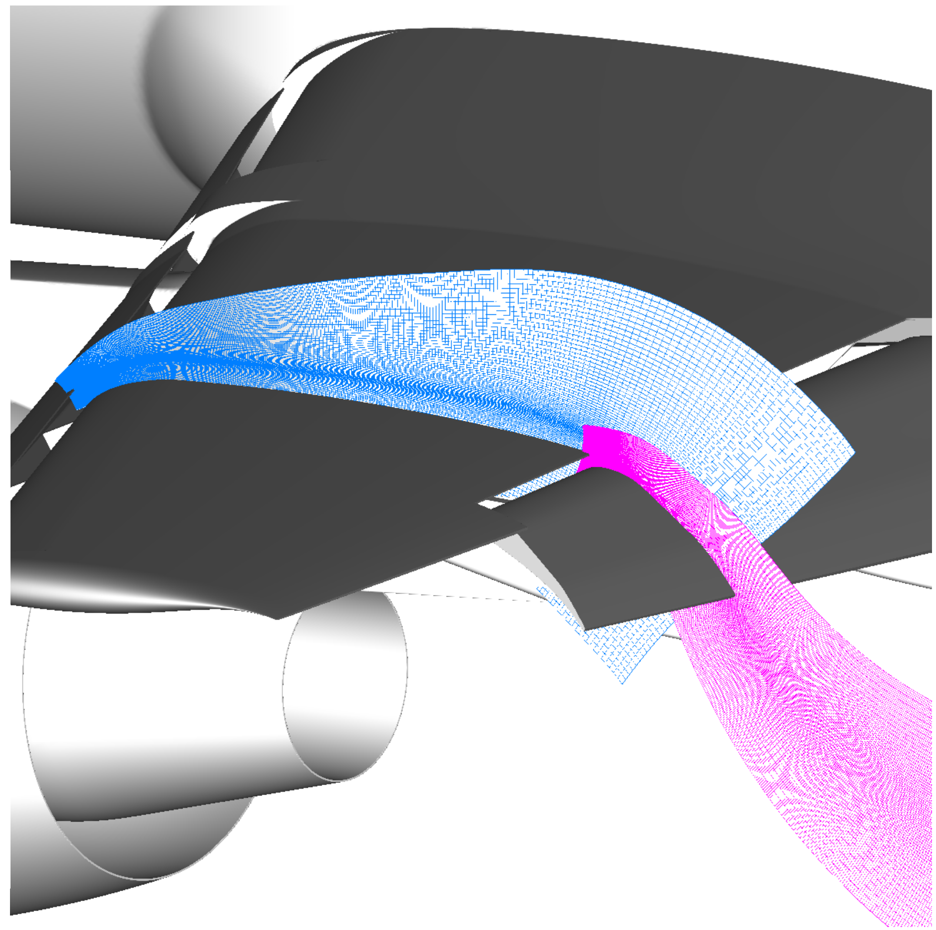

Final "Geometric" Wake Grids

Differences Between Mesh Paradigms

- Overset meshes allow more control in areas such as the leading edges of the elements
- Unstructured mesh can capture small geometrical features with less complexity in the grid

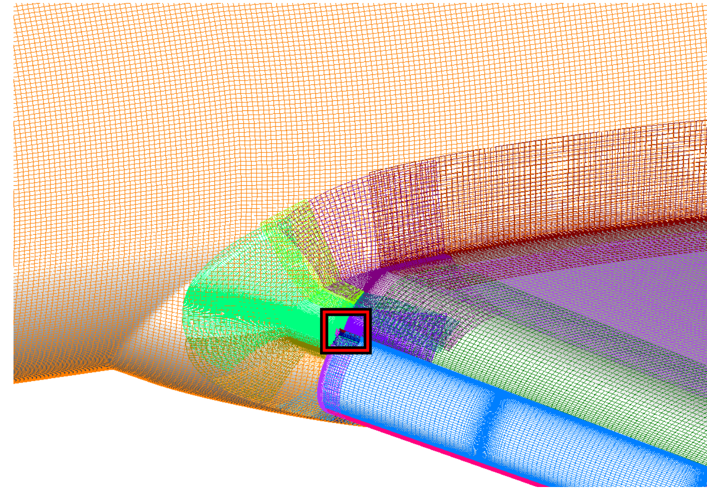

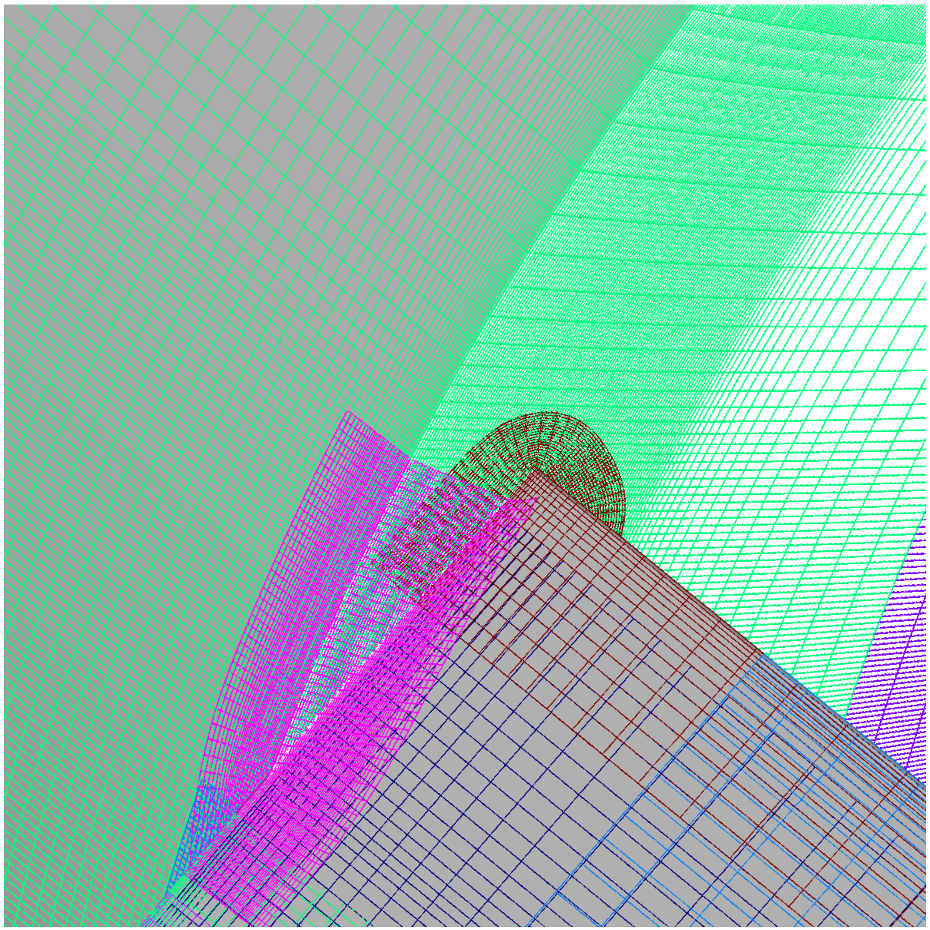

Inboard Slat-Wing Junction (Overset)

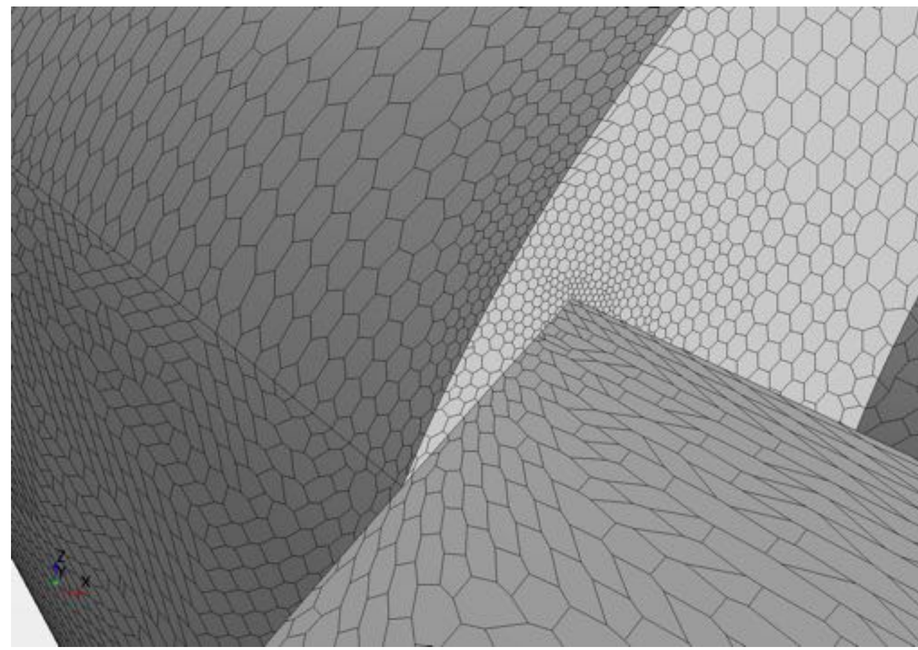

Inboard Slat-Wing Junction (Unstructured)

LAVA Modified Implicit Hole Cutting (MIHC) Procedure

- First the DCF routines in OVERFLOW are used to provide a minimum hole cut and ensure that the required number of fringe layers are available (with minimum hole) for the flow solver (double fringe in this case)
- The global wall-distance is also computed and stored to file
- Next the MIHC code is applied to the overset grid system with the minimum holes cut

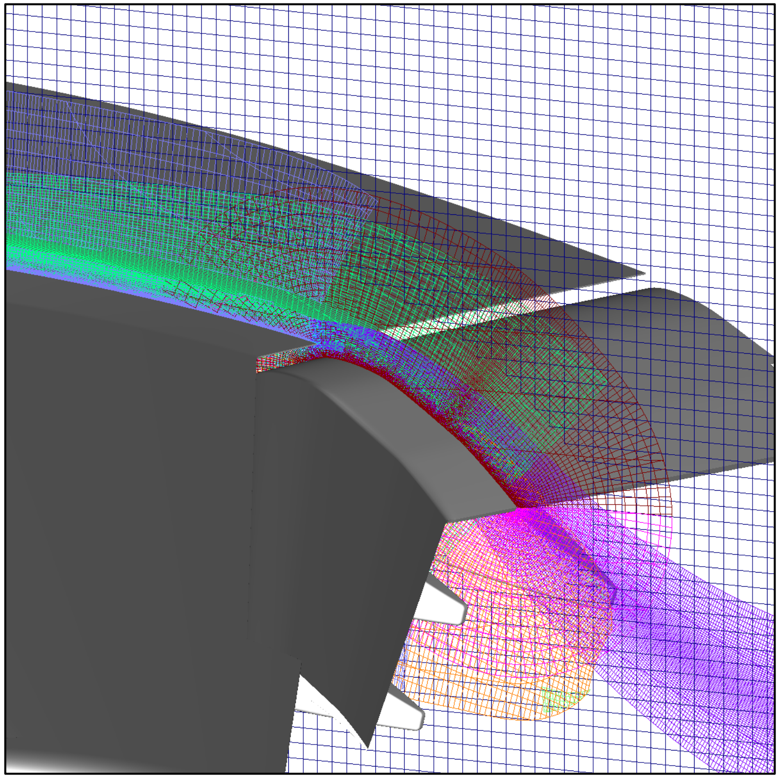

Minimum Hole

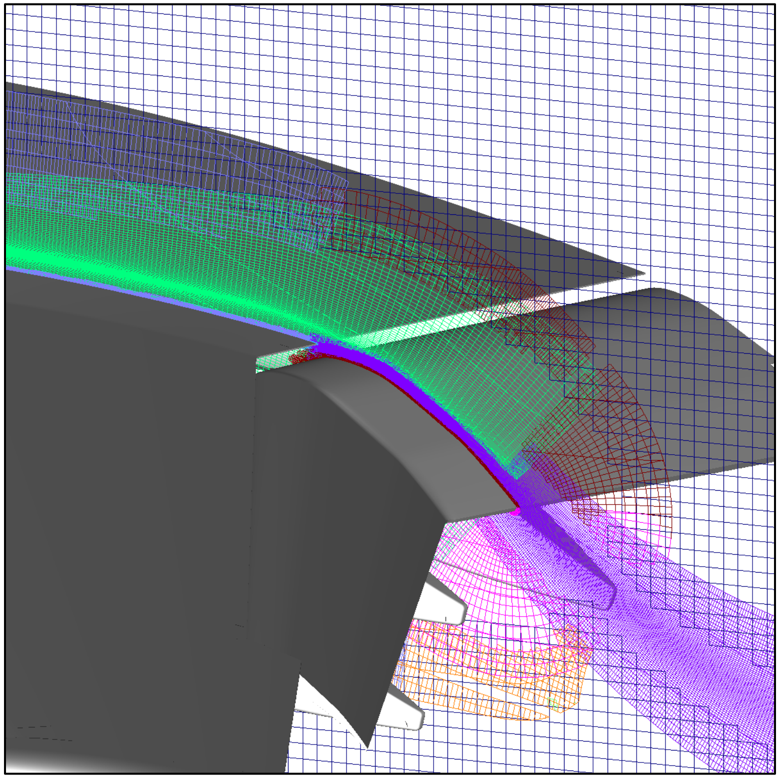

Final Hole

Wake Grids

- The different connectivity codes incorporated the wake grids differently

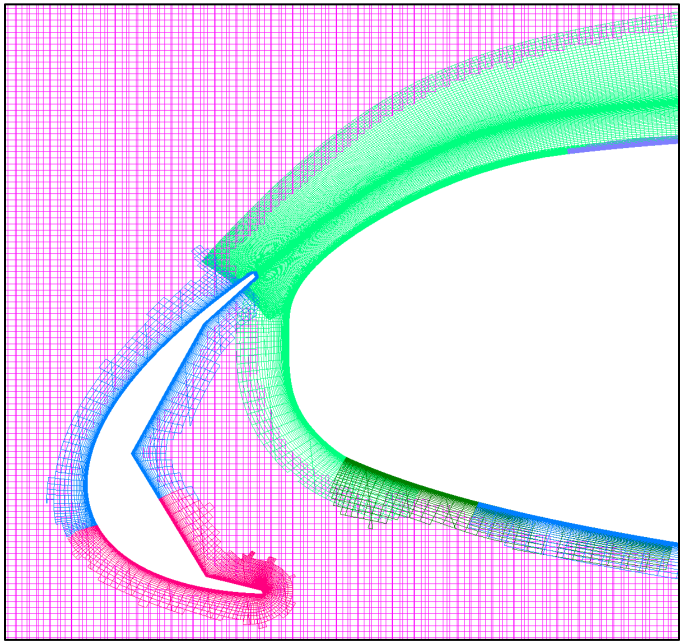

MIHC Wake Grids

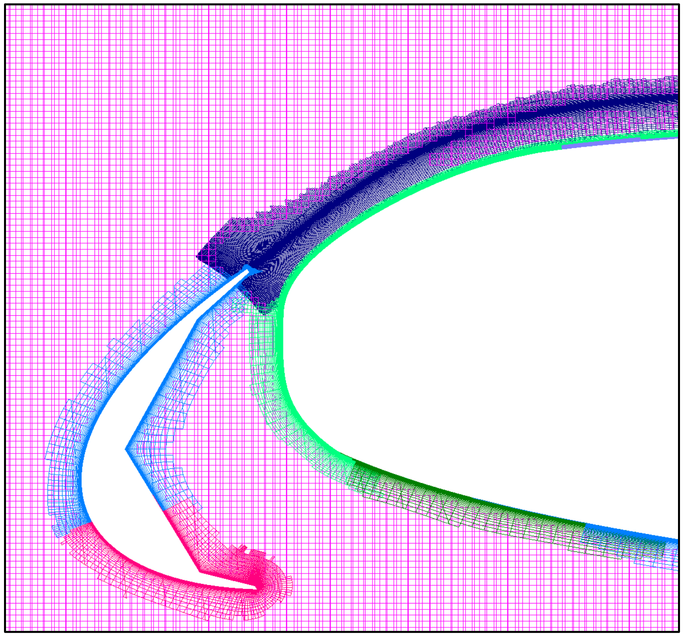

Peg5 Wake Grids

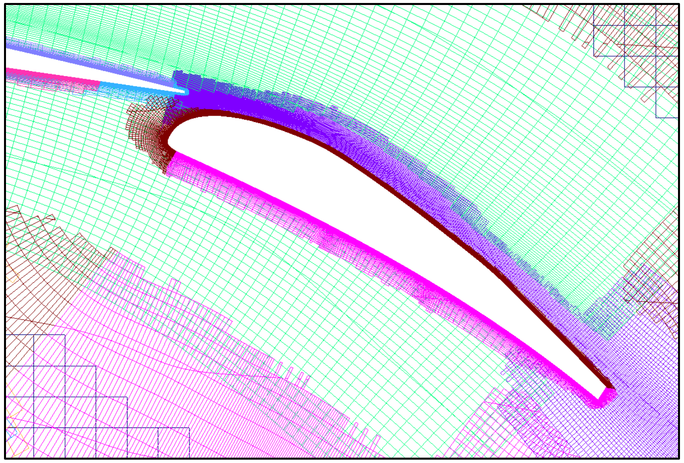

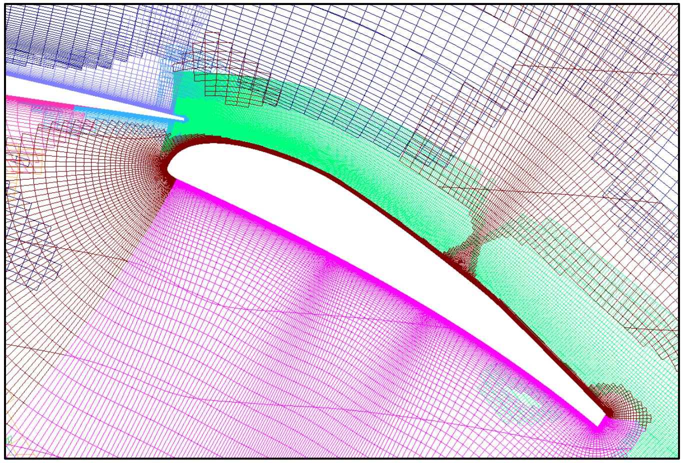

HL-CRM (Case 1) Topology Difference

- Saw larger than expected solution decoupling in the slat Cp plots
- First suspicion was that the surfaces were not identical but they were made by splitting one surface mesh
- Different volume grid generation methods
- Leads to a different amount of solution decoupling at the grid interfaces

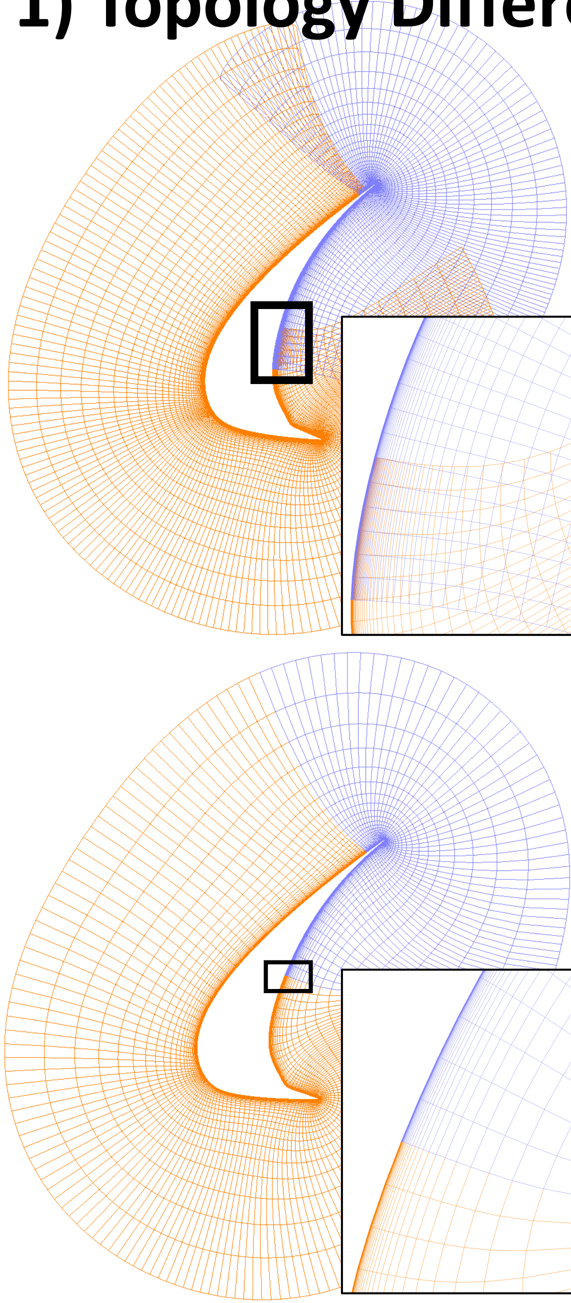

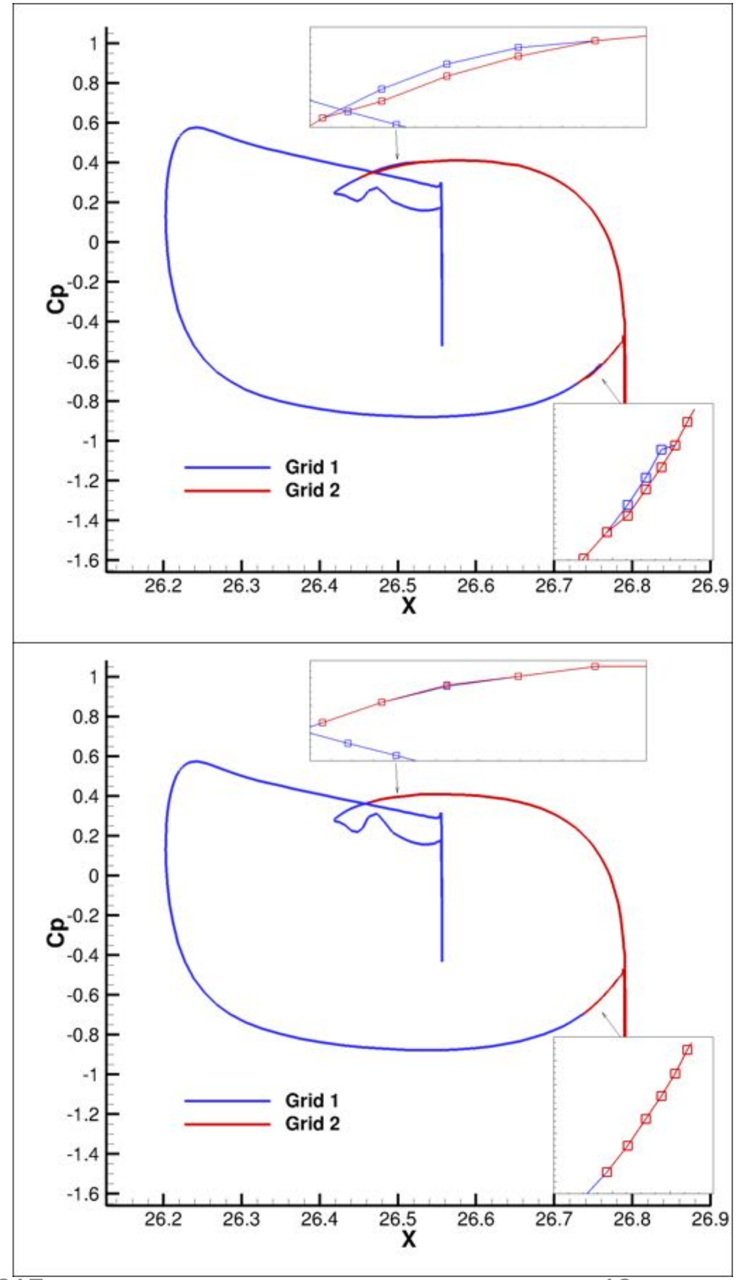

HL-CRM (Case 1) Topology Difference

- Slide showing improvement as the mesh is refined

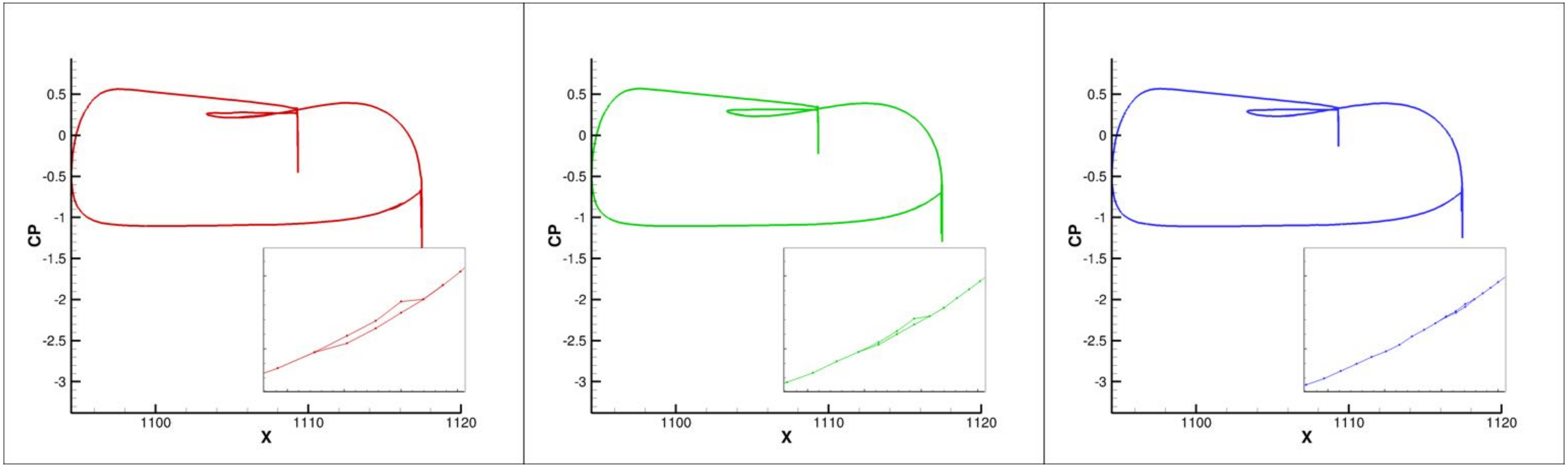

HL-CRM (Case 1a) Grid Convergence Effect

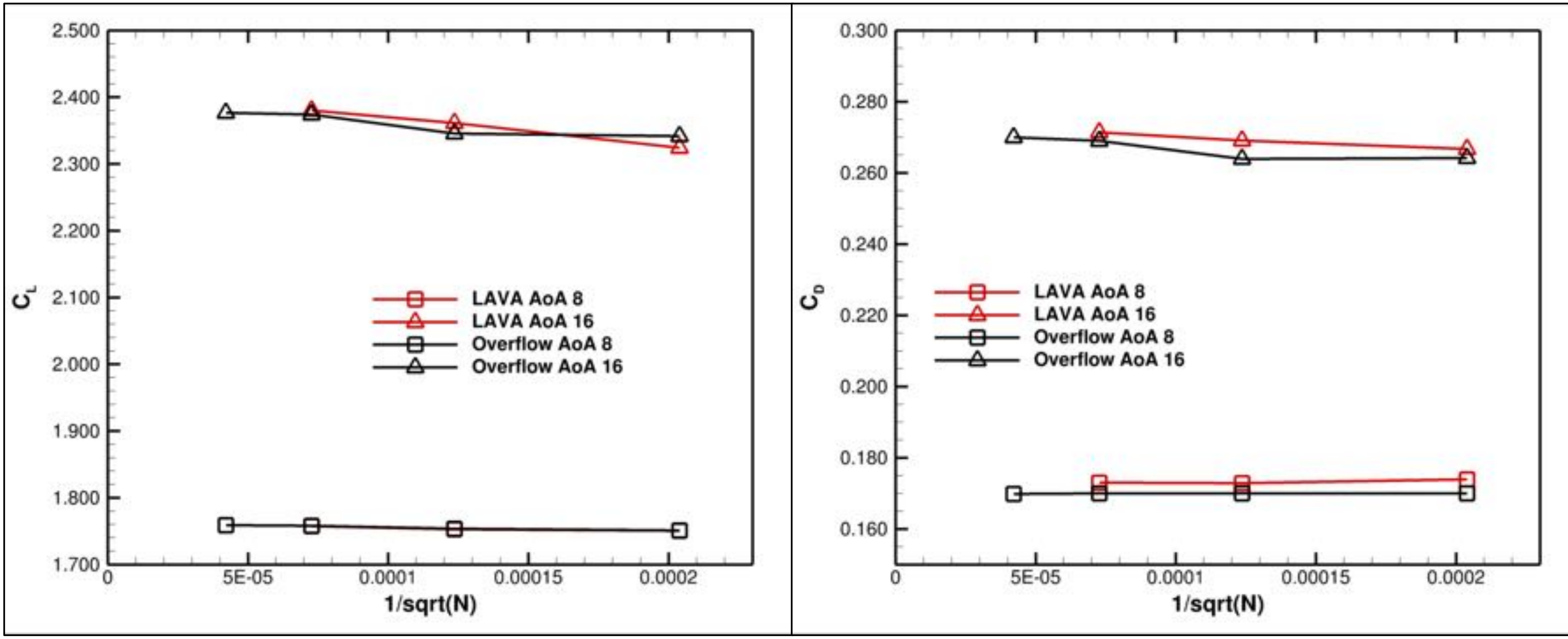

- Lift is converging well at both angles and has converged to an almost identical value from both solvers at both angles
- Drag is converged at α=8 and is converging at α=16
- The solvers are within 10 drag counts of each other at both angles of attack

JSM (Case 2a) Force and Moment Comparisons

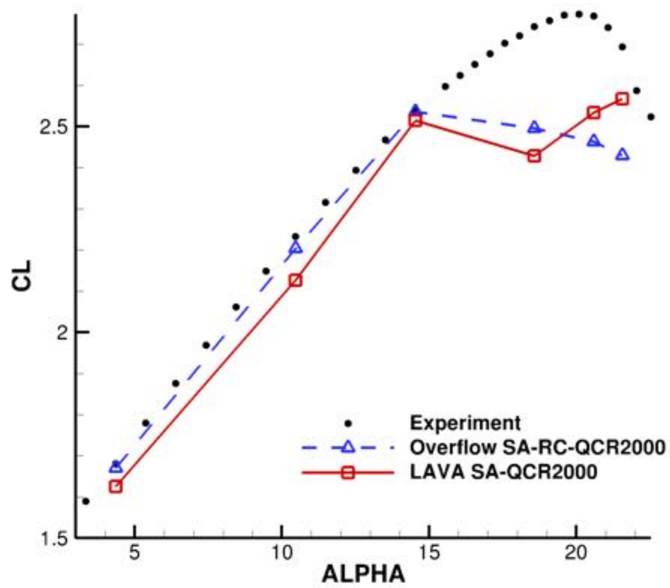

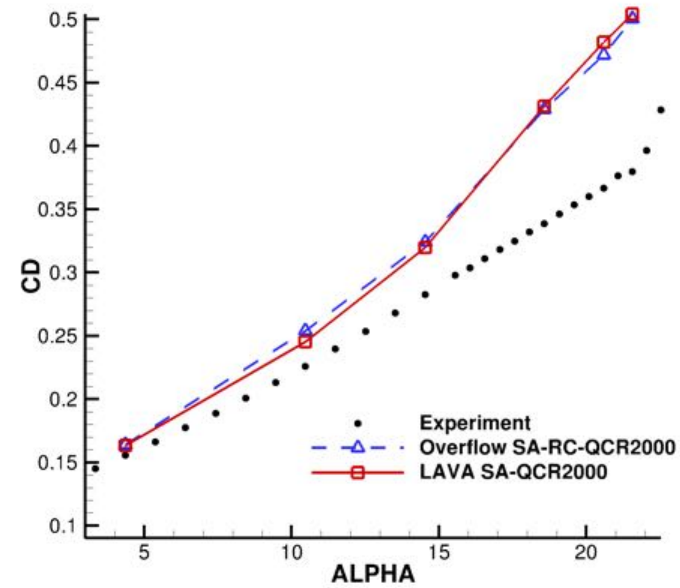

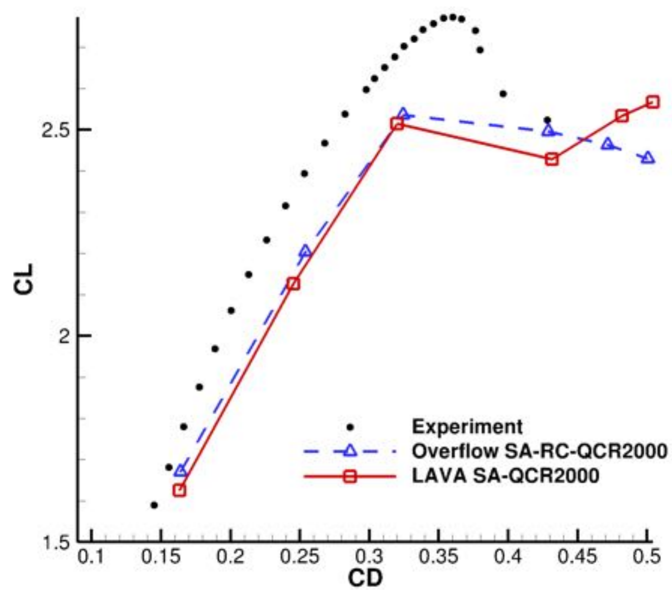

JSM (Case 2a) Cp Comparisons D-D

- At both angles of attack the flap is fairly different between the two solvers
- At α=18.58° the difference in the solutions at the flap becomes even more pronounced
- Overflow appears to match the peak better and LAVA appears to match better in the recovery region

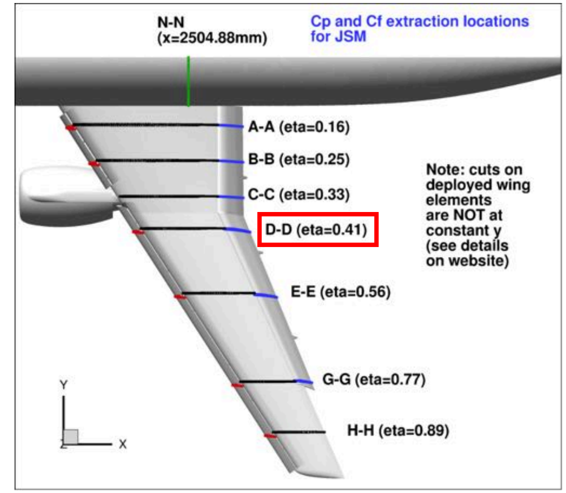

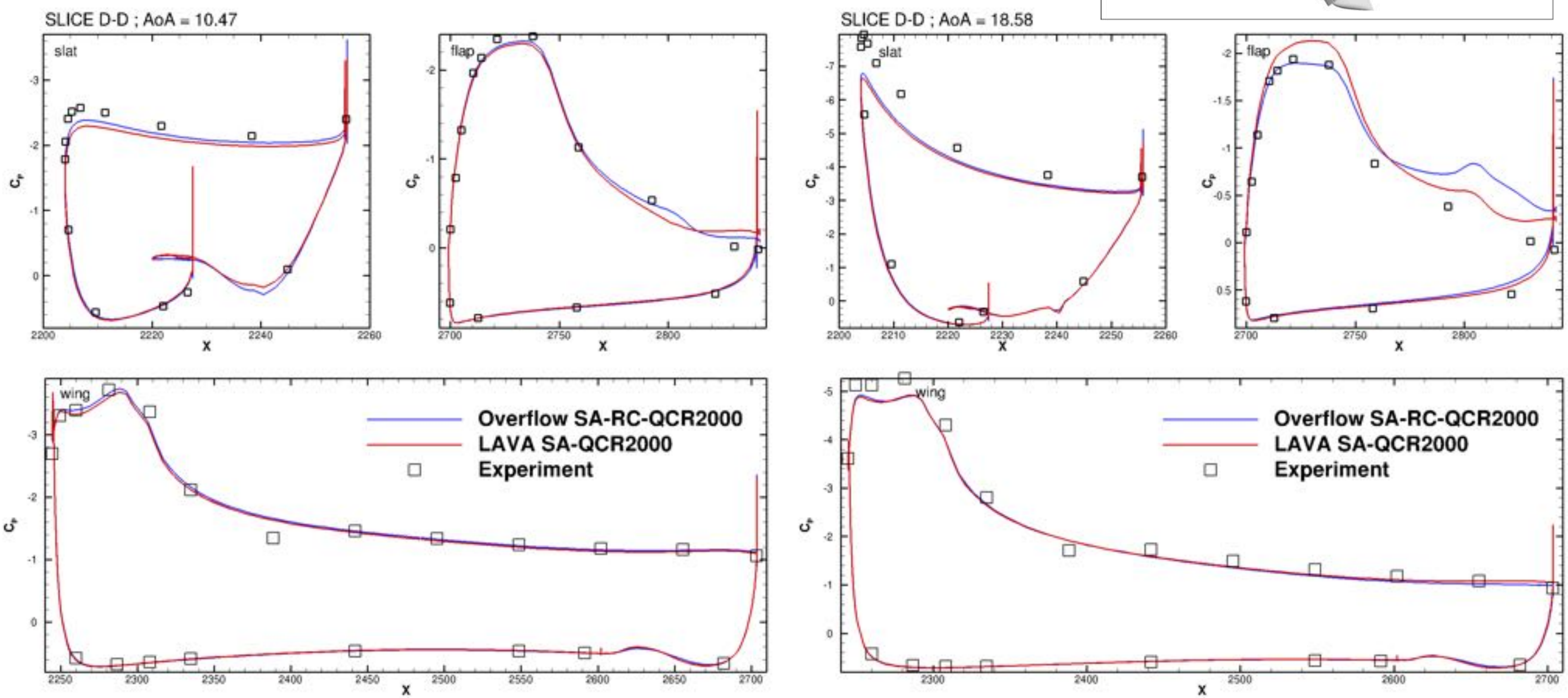

JSM (Case 2a) Cp Comparisons G-G

- The differences between the solvers is more pronounced at this station
- At the higher angle of attack the differences become more pronounced
- On the flap LAVA is closer to the experiment at the peak and Overflow is closer at the TE

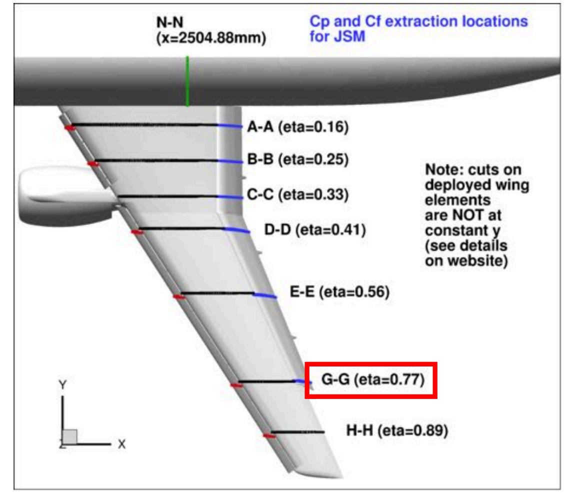

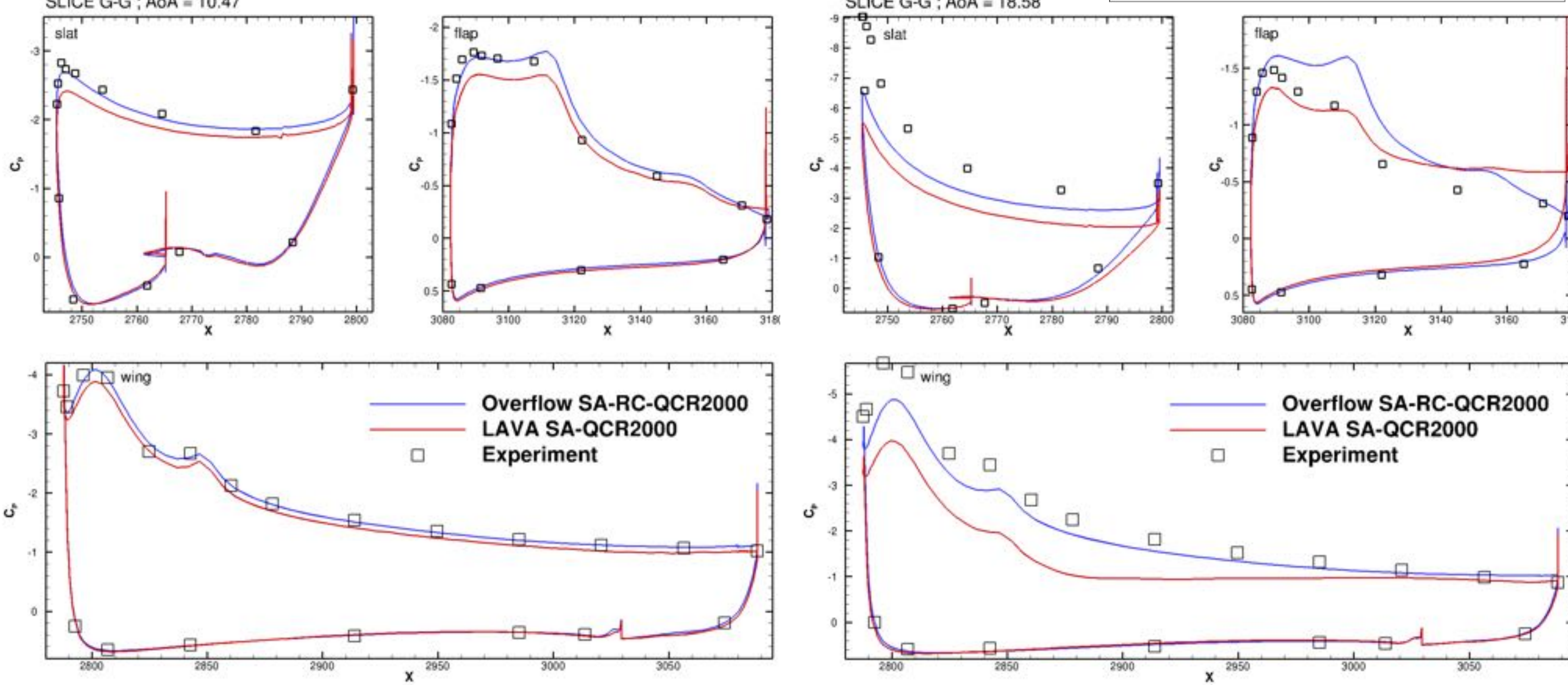

JSM (Case 2c) Force and Moment Comparisons

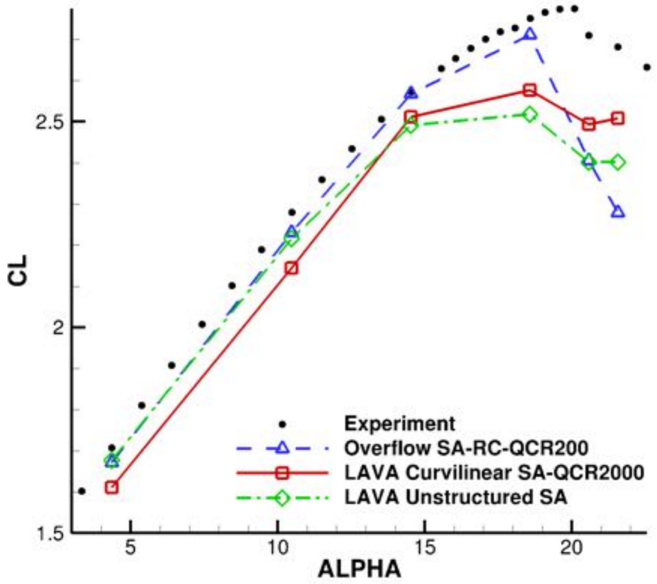

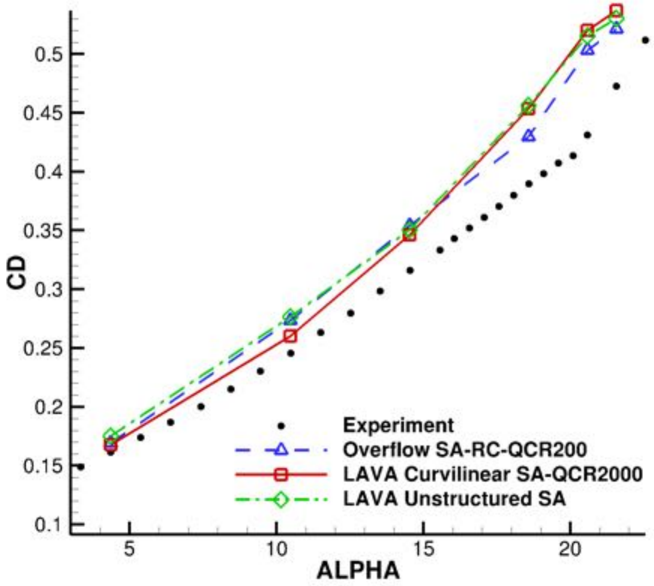

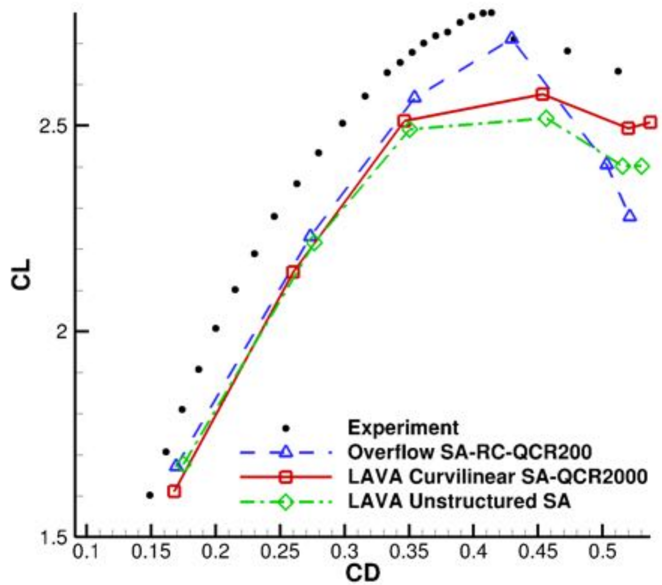

JSM (Case 2c) Cp Comparisons D-D

- At the lower angle of attack Overflow is more closely matching the experimental data but at the higher angle of attack LAVA more closely matches the experiment
- On the slat Overflow and the LAVA Unstructured result are closer to the experiment at both angles of attack

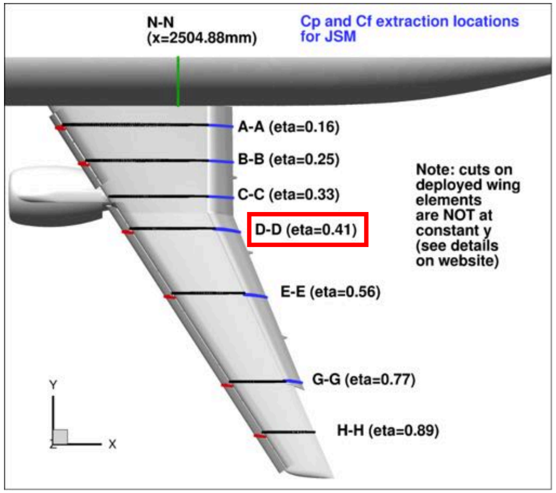

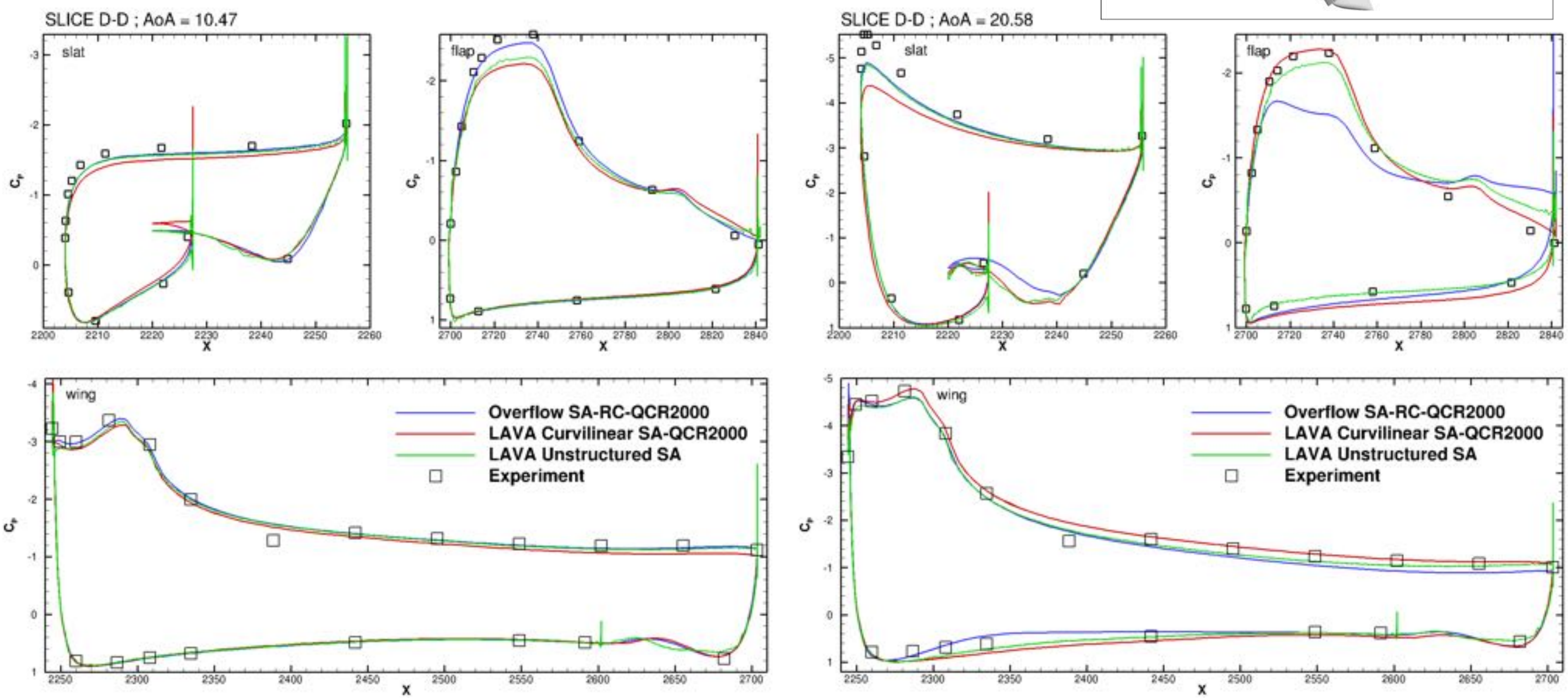

JSM (Case 2c) Cp Comparisons G-G

- At the low angle on the flap we see a similar trend as before; Overflow is closer to the experiment near the peak but LAVA is closer in the recovery region
- At the high angle of attack all of the solvers have similar predictions

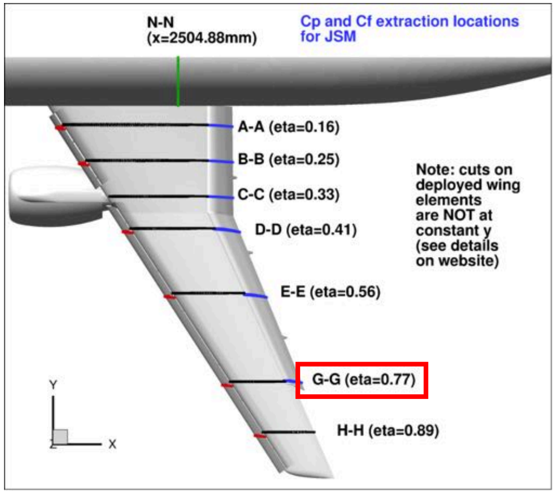

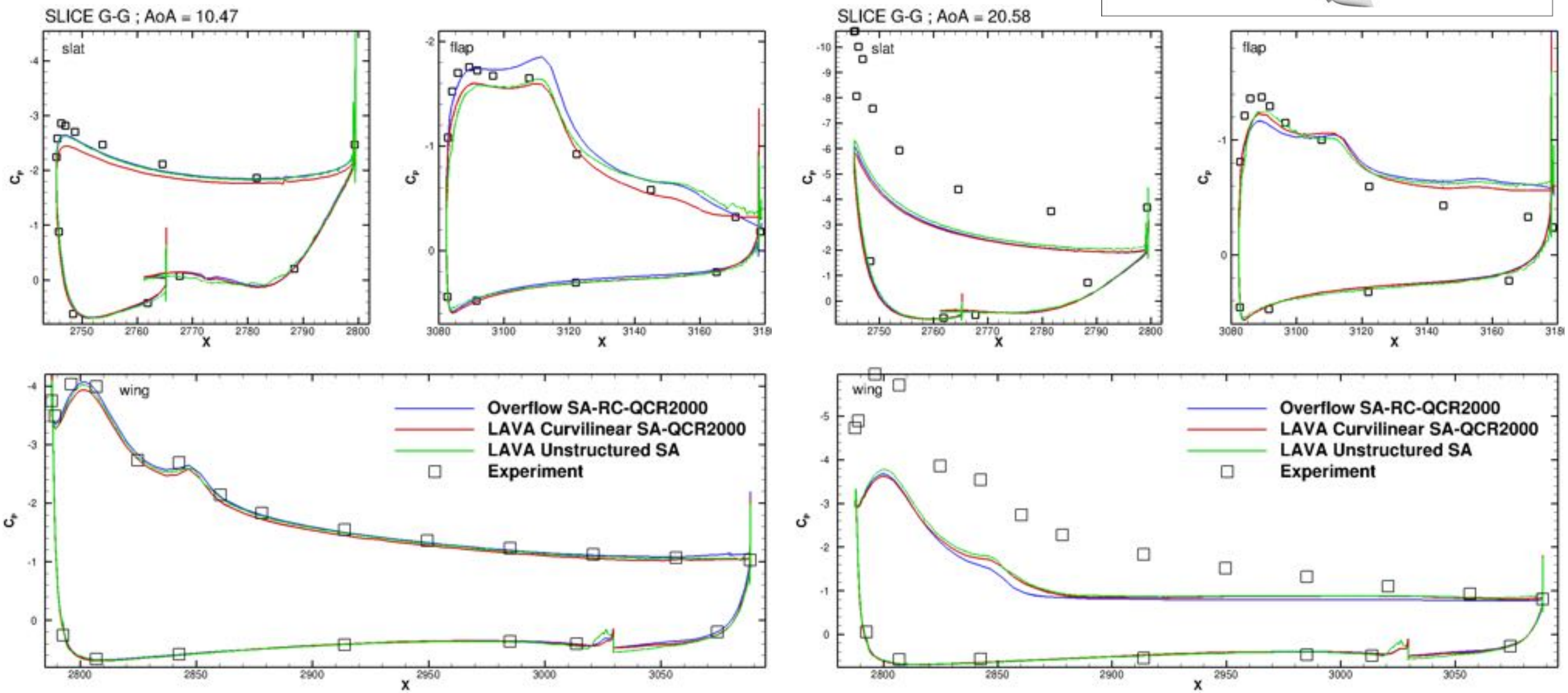

Run Time and Resource Usage Comparison

- Insert table with representative run times and resources for Case 2c

Summary

- Generated the committee overset grid system for the JSM model (Case 2a and Case 2c)
- Observed some unexpected solution decoupling in Case 1 due to the way the grids had been generated
- LAVA force results agreed well with the Overflow results for Case 1
- The Cp and Force results are similar between all of the solvers for both Case 2a and Case 2c
- The differences within the results can be mostly attributed to the differences in the turbulence models, specifically the inclusion of RC

Acknowledgements

- Transformational Tools and Technologies (TTT) project under ARMD
- NAS for computer time on Pleiades